nature communications

Article

https://doi.org/10.1038/s41467-025-56983-8

On the way to diploidization and unexpected ploidy in the grass *Sporobolus* section *Spartina* mesopolyploids

Received: 2 May 2024

Accepted: 6 February 2025

Published online: 26 February 2025

Check for updates

Armel Salmon[1,7], Yan Hao[2,7], Morgane Milin[1,7], Oscar Lima[1], Armand Cavé-Radet[1], Delphine Giraud[1], Corinne Cruaud[3], Karine Labadie[3], Benjamin Istace[4], Caroline Belser[4], Jean-Marc Aury[4], Patrick Wincker[4], Bo Li[2,5] ✉, Lin-Feng Li[6] ✉ & Malika Ainouche[1] ✉

Plant history is characterized by cyclical whole genome duplication and diploidization with important biological and ecological consequences. Here, we explore the genome history of two related iconic polyploid grasses (*Sporobolus alterniflorus* and *S. maritimus*), involved in a well-known example of neopolyploid speciation. We report particular genome dynamics where an ancestral *Sporobolus* genome (n = 2x = 20) duplicated 9.6-24.4 million years ago (MYA), which was followed by descending dysploidy resulting in a genome with an unexpected base chromosome number (n = 15). This diploidized genome duplicated again 2.1-6.2 MYA to form a tetraploid lineage (2n = 4x = 60), thus reshuffling the ploidy of these species previously thought hexaploids. We also elucidate the mechanism accompanying the speciation between *S. maritimus* (2n = 60) and *S. alterniflorus* (2n = 62), resulting from chromosome restructuring, and identify key adaptive genes in the corresponding regions. This represents critical findings to decipher molecular mechanisms underlying species expansion, adaptation to environmental challenge and invasiveness.

Recent efforts have been made to examine the critical role of cyclical whole genome duplication (WGD), or polyploidization, in plants[1], representing springboards for genome dynamics and phenotypic novelties[2–4]. Accumulating evidence of superimposed rounds of WGD, followed by diploidization and genome downsizing[5,6] is now documented across the history of all plant lineages. Both short-term and long-term effects of polyploidy have important implications for species adaptation, survival[7] and functional diversification[8]. Polyploidy (particularly in hybrid context, i.e. allopolyploidy) has been shown to increase stress tolerance[9,10] and most invasive species appear to be recent polyploids[11,12]. Thus, documenting the genome history, phylogenetic context and mode of formation of polyploids is fundamental

[1]UMR CNRS 6553 ECOBIO University of Rennes, Campus de Beaulieu, 35042 Rennes, Cedex, France. [2]State Key Laboratory of Wetland Conservation and Restoration, National Observations and Research Station for Wetland Ecosystems of the Yangtze Estuary, Ministry of Education Key Laboratory for Biodiversity Science and Ecological Engineering, and Institute of Eco-Chongming, School of Life Sciences, Fudan University, Shanghai, China. [3]Genoscope, Institut François Jacob, CEA, CNRS, Univ Evry, Université Paris-Saclay, Evry 91057, France. [4]Génomique Métabolique, Genoscope, Institut François Jacob, CEA, CNRS, Univ Evry, Université Paris-Saclay, Evry 91057, France. [5]State Key Laboratory for Vegetation Structure, Functions and Construction, Ministry of Education Key Laboratory for Transboundary Ecosecurity of Southwest China, Yunnan Key Laboratory of Plant Reproductive Adaptation and Evolutionary Ecology, Institute of Biodiversity, School of Ecology and Environmental Science and the Southwest United Graduate School, Yunnan University, 650500 Kunming, China. [6]State Key Laboratory of Biocontrol, Guangdong Provincial Key Laboratory of Plant Stress Biology, School of Life Sciences, Sun Yat-sen University, Guangzhou 510275, China. [7]These authors contributed equally: Armel Salmon, Yan Hao, Morgane Milin. ✉e-mail: Bool@ynu.edu.cn; lilinfeng@mail.sysu.edu.cn; malika.ainouche@univ-rennes.fr

to our understanding of biological processes. Of particular interest is the process of diploidization that shapes most modern plant genomes and that is still poorly understood.

The former grass genus *Spartina* Schreb. (included in genus *Sporobolus*, section *Spartina*[13]) is a model in evolutionary ecology[14–16]. Recurrent hybridization and polyploidization events resulted in species of various ploidy levels[17]. Reticulate evolution and WGD represent major genomic determinants that shaped the physiological, biological and ecological traits of these species following genetic, epigenetic and transcriptomic evolution[18–25]. Section *Spartina* contains species that are considered as ecosystem engineers in coastal saltmarshes, and some of which are highly invasive, such as *Sporobolus alterniflorus* (*syn. Spartina alterniflora*, smooth cordgrass), that is recognized as indigenous across a span of over 100 degrees of latitude along the Atlantic coastline of the Americas and expanded outside its native range on different continents, particularly in China where it is now distributed across a large latitudinal gradient[15,26,27]. In their native ranges, these species are highly valued; they tolerate a large range of saline, anoxic and sulfidic soils[28,29] and are important for coastal reclamation and restoration[30,31]. Of particular interest is the well-known model of neopolyploidy involving hybridization in Western Europe between the introduced American *S. alterniflorus* (2n = 62) as female parent and the native *S. maritimus*, (*syn. Spartina maritima*, 2n = 60) during the 19th century[14,32]. Genome duplication of the hybrid *S. x townsendii* (2n = 62) resulted in the successful allopolyploid species *Sporobolus anglicus*, (*syn. Spartina anglica*, 2n = 124)[33], which has rapidly colonized European saltmarshes and is now introduced in several continents[14]. This system is an excellent model to explore the consequences of hybridization and WGD at various evolutionary time scales, in neo- and meso-polyploidy contexts[24].

Variable base chromosome numbers (x = 6, 8, 9, 10) were reported in the *Sporobolus* genus[13,34]. Comparative studies[35,36] suggested the base chromosome number in *Spartina* as x = 10, and subsequently tetraploidy for species with 2n = 40, hexaploidy (6x) for *S. maritimus* and *S. alterniflorus*, dodecaploidy (12x) for *S. anglicus*. Molecular phylogenies revealed that the hexaploids (*S. maritimus*, *S. alterniflorus* and *S. foliosus*) derived from a common ancestor[37,38] that diverged from tetraploids 6-10 million years ago (MYA)[39]. The autopolyploid or allopolyploid nature of this hexaploid clade is still unclear, although more or less divergent duplicated copies of targeted genes from genetic[38,40] or transcriptomic[41] data suggested allopolyploidy without ruling out auto-allopolyploidy.

Here, we provide a reference genome for *S. maritimus* and compare it with *S. alterniflorus*[42], identify their duplicated subgenomes, and explore their evolutionary history. We show how two successive WGD events and evolution of a novel base chromosome number during the last 20 million years have shaped the modern genomes of *S. maritimus* and *S. alterniflorus*, which appear to be tetraploid and not hexaploid as previously thought[11,17]. We elucidate the mechanisms underlying the divergence between *S. maritimus* and *S. alterniflorus ca.* 2.1-6.2 MYA following chromosomal re-patterning that led to their different chromosome numbers (2n = 60 and 2n = 62, respectively). This shed light on the genomic composition of the neopolyploid *S. anglicus*.

Results

Genome assembly

Combining both short and long reads and optical mapping, the *S. maritimus* genome was assembled into 69 scaffolds totalling 1595 Mb with a contig N50 of 34.7 Mb. The genome survey displayed a BUSCO-score of 95.9% of complete retrieval of Embryophyta core genes. A k-mer distribution confirmed the split of homeologous genomes (Supplementary Fig. 1, Supplementary Table 1), with a remnant duplication rate of 53.8%. The *S. maritimus* genome assembly represented 89% of the estimated PI-flow-cytometry genome size (1795 Mb).

The *S. alterniflorus* genome assembly was 1.63 Gb in length with a contig N50 of 28.25 Mb. Chromosome-scale scaffolding was performed using 251.49 Gb (154.29 × genome coverage) paired-end Hi-C short reads, with 1.59 Gb of contigs successfully assigned to 31 pseudomolecules. The contig N50 of the final genome assembly was 18.80 Mb in length.

Read mapping against the assembled genomes indicated homogenous coverage among scaffolds in *S. maritimus* (Supplementary Fig. 2A), as well as among *S. alterniflorus* chromosomes (Supplementary Fig. 2B), which suggests equivalent subgenome dosage in each of these polyploids.

Genome composition

A total of 79,568 and 73,711 protein-coding genes were identified in *S. maritimus* and *S. alterniflorus* respectively. Gene and repeat densities in the *S. maritimus* genome (Fig. 1) were inversely distributed, with a distal gene position on the chromosomes or scaffolds as reported for the *S. alterniflorus* genome[42]. An overall collinearity between *S. maritimus* and *S. alterniflorus* genomes is represented in Fig. 1. In *S. maritimus*, 946 Mb (59.3% of the genome) were annotated as repeated sequences, and 1,192.78 Mb (73.13%) in the *S. alterniflorus* genome. In both species, long terminal repeats (LTR) transposable elements were relatively abundant (43% in *S. maritimus* and 52% in *S. alterniflorus*) with *Gypsy* and *Copia* elements accounting for 32% and 11% of the *S. maritimus* genome, respectively, and 35% and 17% of the *S. alterniflorus* genome, respectively (Supplementary Table 2). Similar bursts were observed in both species for *Copia* elements (one *ca.* 7 MY -old burst) and *Gypsy* elements (two bursts *ca.* 5 and 10 MY -old respectively, Supplementary Fig. 3). Tandem repeat annotation (Supplementary Fig. 4) allowed the detection of a High Order Repeat (HOR) of 147 bp shared by the two species within *S. alterniflorus* chromosomes and *S. maritimus* scaffolds, representing a putative centromeric satellite sequence. Some chromosomes of *S. alterniflorus* appeared depauperate in this 147 bp-putative centromeric repeat, particularly chromosome 31. Some *S. maritimus* scaffolds appeared to assemble single chromosome arms (from a distal/telomeric region to putative centromeric repeats). A second HOR of 169 bp maps at chromosomes and scaffolds distal regions. The 370-bp satellite repeat, more abundant in *S. alterniflorus* than in *S. maritimus* (Supplementary Table 2), appeared mostly distributed in distal chromosomal regions (Supplementary Fig. 5). *S. alterniflorus* chromosome 24 was particularly enriched with this repeat on both chromosome arms.

Divergence and molecular dating between homeologs

Homology searches revealed the presence of four subgenomes (A1-A2 / B1-B2) within both *S. maritimus* (Supplementary Fig. 6A) and *S. alterniflorus* (Supplementary Fig. 6B). Equivalent (1:1:1:1) subgenome dosage is suggested from read coverage (Supplementary Fig. 2). The species comparison confirmed the shared presence of these two WGD events that resulted in the presence of two levels of divergence (Fig. 2): A versus B and A1-A2 or B1-B2 (Supplementary Fig. 7). Fifteen homeogroups were defined based on highest similarities between genomic sequences (Fig. 3), suggesting the presence of two sets of 15 homeologous chromosomes in *S. alterniflorus* and *S. maritimus*.

Distribution of synonymous substitutions (Ks) between duplicated gene pairs within genomes (Fig. 2A) revealed three peaks in both *Sporobolus* genomes and only one in rice. The most recent event (WGD2) is represented by a Ks peak of 0.047 ± 0.02 (3.6 MYA, range = 2.1–5.3 MYA) in *S. maritimus*, and 0.06 ± 0.021 (4.6 MYA, range = 3.0–6.2 MYA) in *S. alterniflorus*, which would indicate that the WGD2 event occurred between 2.1–6.2 MYA. The other peak, referred to as WGD1 event, is represented by a Ks mode of 0.229 ± 0.088 (17.6 MYA, range = 10.5–24.4 MYA) in *S. maritimus* and 0.194 ± 0.069 (14.9 MYA, range = 9.6–20.2 MYA) in *S. alterniflorus*, which suggests that this WGD1 event occurred sometimes between 9.6 and 24.4 MYA. The third

https://doi.org/10.1038/s41467-025-56983-8

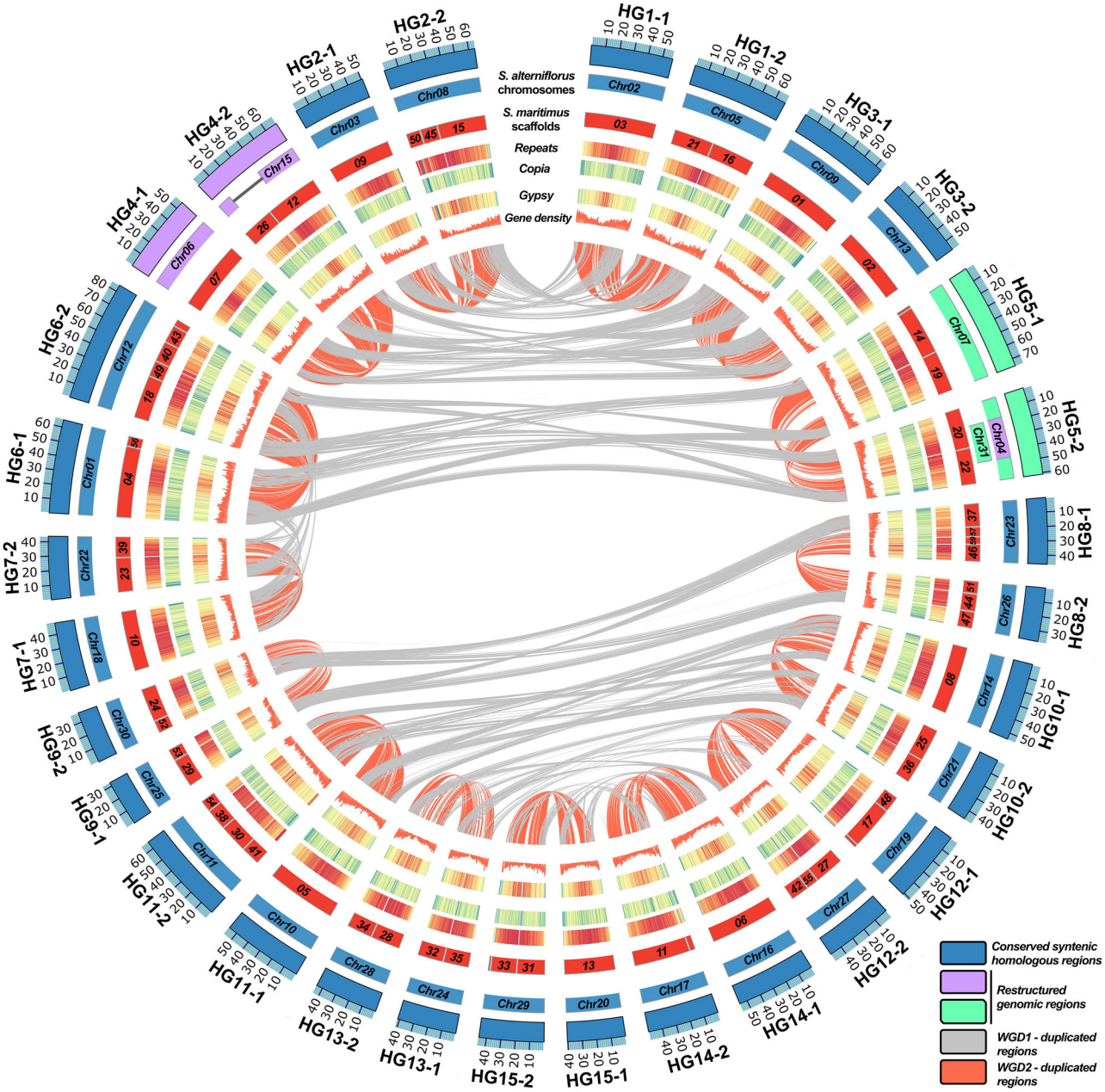

Fig. 1 | Synteny and genomic feature distribution of *S. maritimus* and comparison with *S. alterniflorus*. The external circle represents the genomic reference corresponding to 30 conserved homologous genomic regions (HG) between *S. maritimus* and *S. alterniflorus*. Restructured HGs are represented in purple and light green. The grey line for *S. alterniflorus* Chr15 corresponds to the excised syntenic region forming part of Chr04. Repeat, LTR-*Copia*, and LTR-*Gypsy* densities by 100kb-windows are represented as log-scale heatmaps from blue (minimum values) to red (maximum values), gene densities were calculated by 100kb-windows. Syntenic blocks between HGs on the basis of 57,724 gene orthologs. Red and grey links correspond to duplicated syntenic regions resulting from WGD2, and WGD1, respectively. Source data are provided as a Source Data file.

peak (*rho* WGD) showed a Ks mode of ~0.672, 0.748 and 0.558, in *S. maritimus*, *S. alterniflorus* and *O. sativa* respectively, estimating this event to have occurred between 31–78 MYA. The Ks distribution of homologous gene pairs between species (Fig. 2B) revealed that only one peak was shared between the two *Sporobolus* species and the rice genome (Fig. 2B), while three WGD events were shared between *S. maritimus* and *S. alterniflorus*. The Ks distribution analysis of two homeogroups detected in *S. alterniflorus* and *S. maritimus* genomes (Supplementary Fig. 7) confirmed that the copies 1 and 2 in each A and B subgenomes derived from a unique shared WGD event. The peak with Ks value mode of 0.061 ± 0.027 (4.7 MYA, range = 2.6–6.8 MYA) reflected both subgenome divergence following WGD2 and between *S. alterniflorus* and *S. maritimus*, indicating that speciation might have occurred relatively soon after WGD2. Nucleotide identities between *S. maritimus* and *S. alterniflorus* orthologous genes ranged between 96.6 and 98.7% (Supplementary Fig. 8).

Karyotype evolution between *S. maritimus* and *S. alterniflorus*

The search for syntenic blocks between *S. maritimus* and *S. alterniflorus* genomes allowed us to reconstruct *S. maritimus* pseudochromosomes (Fig. 1). The karyotype comparison revealed chromosomal restructuring involving homeogroups 4 and 5 and resulting in the additional chromosome 31 in *S. alterniflorus* (Fig. 3A). A portion of the *S. maritimus* scaffold 7 is missing on the corresponding

https://doi.org/10.1038/s41467-025-56983-8

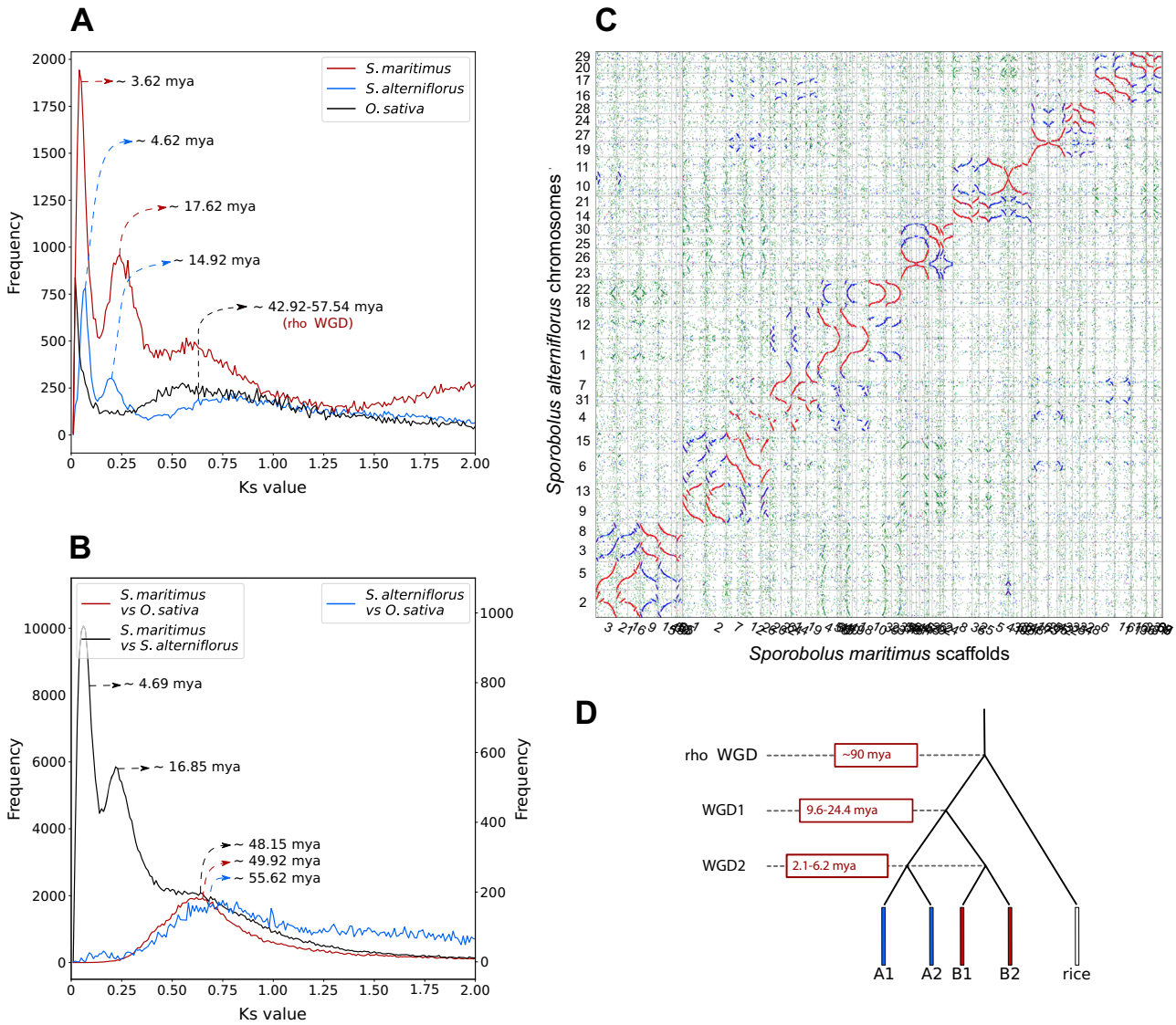

Fig. 2 | Intragenomic and intergenomic comparisons. A Ks distributions within *S. maritimus* (red; *N* = 99,442 compared gene pairs), *S. alterniflorus* (blue; *N* = 33,827) and *O. sativa* (black; *N* = 23,896) genomes; **B** Ks distributions between *S. maritimus* and *S. alterniflorus* (black; *N* = 356,305), *S. maritimus* and *O. sativa* (red; *N* = 117,035), *S. alterniflorus* and *O. sativa* (blue; *N* = 19,881). **C** Dotplot comparisons between *S. maritimus* and *S. alterniflorus* assembled genomes. Ks values were used to color the dots: red (0.01–0.1), blue (0.1–0.3) and green (0.3–3). *S. maritimus* scaffolds are ordered as following: 3, 21, 16, 9, 15, 45, 50, 58, 65, 1, 2, 7, 12, 26, 20, 22, 64, 14, 19, 4, 56, 60, 43, 40, 49, 18, 10, 39, 23, 37, 57, 59, 46, 51, 44, 47, 53, 29, 52, 24, 8, 36, 25, 5, 41, 30, 62, 38, 54, 48, 17, 63, 27, 55, 42, 32, 35, 34, 28, 6, 11, 61, 13, 66, 33, 31, 67, 68, 69. **D** Divergence time estimates between subgenomes resulting from WGD1 and WG2 events. Source data are provided as a Source Data file.

homologous chromosome 15 of *S. alterniflorus* and has been translocated into chromosome 4. Additionally, on the corresponding homologous chromosome 4, portions of the scaffolds 20 and 22 of *S. maritimus* were absent and were homologous to the additional chromosome 31 in *S. alterniflorus* (Fig. 3B). In silico detection of HORs, showed that all homologous *S. alterniflorus* chromosomes and *S. maritimus* scaffolds displayed central 147 bp-long HOR and distal 169 bp-long HORs, except *S. alterniflorus* chromosome 31 which was lacking of 147 bp-HORs but was enriched in 370 bp-long HORs (Supplementary Fig. 9).

We compared annotated genes of *S. alterniflorus* chromosome 31 with genes from corresponding restructured portions of *S. maritimus* scaffolds 20 and 22 (Fig. 4, Table 1, Supplementary Data 1). Compared to the whole genome where the majority of the GO terms were shared, the restructured regions demonstrate functional divergence between the two species (Fig. 4, Table 1). In addition, the restructured region of *S. maritimus* appeared to be enriched in several biological functions of adaptive interest such as reproduction (pollen tube development), defense (chalcone biosynthetic process) or stress tolerance (lipid biosynthetic process).

Discussion

S. maritimus and *S. alterniflorus* are two iconic polyploid species in ecology and evolutionary biology[16]. In spite of their interest as a model system to explore the consequences of hybridization and WGD in natural populations[11,14,15], little is known about their origin and the nature of their polyploid genome. The comparative analysis of these genomes enhanced our understanding of their common history characterized by successive WGD events and divergence following speciation, and provided insights into the mechanisms involved in the ongoing genome dynamics and diploidization processes in polyploid plants. With 2n = 60 and 62 chromosomes, respectively, *S. maritimus* and *S. alterniflorus* were considered as hexaploid species (with one extra-chromosome pair in *S. alterniflorus*), according to the established base chromosome number x = 10 in the *Spartina* clade[36]. This was consistent with polyploid series reported in *Spartina*, suggesting

https://doi.org/10.1038/s41467-025-56983-8

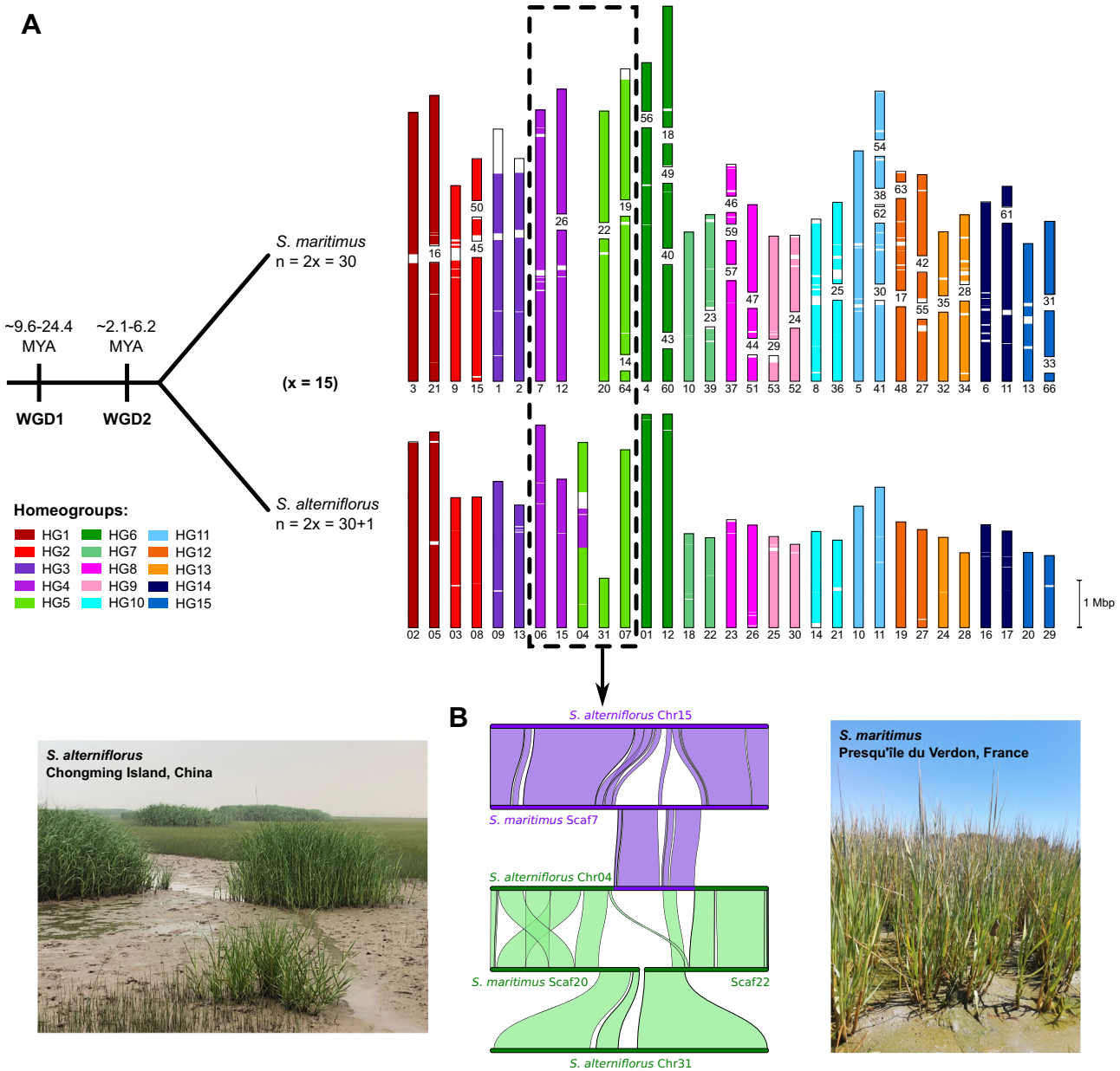

Fig. 3 | Chromosome restructuring between *S. maritimus* (*n* = 30) and *S. alterniflorus* (*n* = 31). A Species karyotypes ("Chromosome lengths" are represented as the sum of genic regions). Translocation between Chr15 and Chr04 led to Chr31 in *S. alterniflorus* chromosomes following WGD2 (*ca.* 2.1-6.2 MYA) – the involved orthologous regions are framed by dotted lines. **B** Focus on syntenic orthologous blocks between *S. maritimus* and *S. alterniflorus* genomic regions affected by the translocation leading to the additional *S. alterniflorus* Chr31.

that hexaploids most likely derived from tetraploids with 2n = 40[17] in the last 6–10 MYA[39]. No diploid species are known among the 15 perennial species of the *Spartina* clade[43], which suggests that this clade most likely emerged from an already polyploid common ancestor.

Considering the propensity of interspecific hybridization among species of the *Spartina* clade and results from duplicate gene phylogenies, an allopolyploid origin of *S. maritimus* and *S. alterniflorus* was suggested[21,38,40]. Supporting this view, two duplicated copies were more frequently detected from transcriptomic data[21,40]. However, the nature of these data did not allow us to discern the actual subgenome dosage nor to rule out strict allohexaploidy (presence of 3 duplicated homeologous genomes e.g. AABBCC structure resulting from 3 divergent progenitors) or autoallopolyploidy (e.g. AAAABB, AAABBB structures resulting from two divergent progenitors). Our whole genome analyses provided a totally different view of the subgenome organization. We clearly showed in both species the presence of four subgenomes (A1, A2, B1, B2) resulting from two successive WGD events. The oldest one (WGD1) dating back to 9.6 to 24.4 MYA led to the formation of A and B subgenomes and the most recent one (WGD2), dating back to 2.1–6.2 MYA, resulted in the less divergent A1-A2 subgenomes and B1-B2 subgenomes. Here we should keep in mind that the estimated divergence times between duplicated gene pairs represent upper age limits of the genome duplication events, as these estimations may actually reflect time elapsed since the divergence between the parental species and/or switch to disomic from polysomic inheritance according to the various ways polyploids may form[44]. The recent duplication event (WGD2) was detected from RNA Seq data in a previous study[40], but the stringent mapping parameters (> 90% identity) employed there did not allow detection of the oldest event.

The presence of four duplicated subgenomes in *S. maritimus* and *S. alterniflorus* as a result of two shared WGD events would suggest an octoploid state, and not hexaploid as previously thought. However, it

https://doi.org/10.1038/s41467-025-56983-8

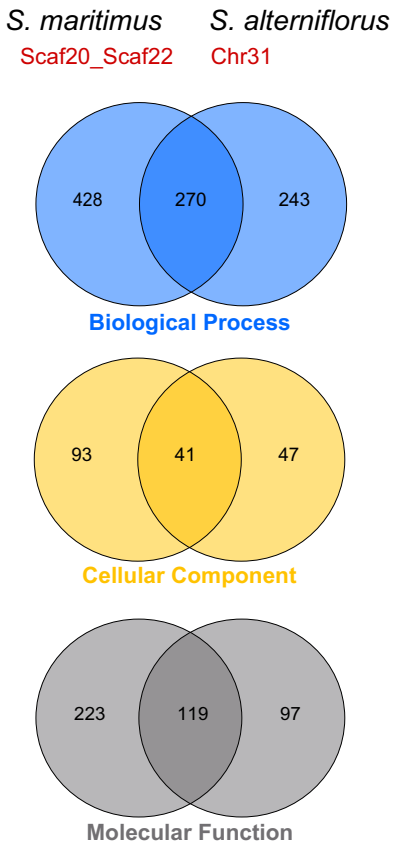

Fig. 4 | Functional divergence in restructured homologous chromosomal regions between *S. maritimus* and *S. alterniflorus*. Venn diagram displaying numbers shared and species-specific GO-terms. Exact (one-sided) *p*-values, *p*-adjusted values (with a cutoff of 0.05), and *q*-values for each term are available in the Supplementary Data 1.

should be pointed out that the presence of 15 (and not 20) homeogroups that were duplicated by WGD2 actually result in a fourfold (4 × 15) genomic structure making the genomes of these species appear as meso-octoploids having evolved into a modern tetraploid state considering the evolved base chromosome number x = 15. *S. maritimus* and *S. alterniflorus* are cytologically diploidized with mostly regular bivalent pairing at meiosis[35]. Such a complex history, where part of the *Spartina* clade has still kept the ancestral base chromosome number x = 10 (2n = 4x = 40, tetraploid clade II[37]), while others (clade I[37], sect. *Spartina* subsect. *Alterniflori*[13]) appear to have evolved a different base chromosome number (x = 15, 2n = 4x = 60), is unexpected, and illustrates the particularly dynamic nature of the polyploidization - diploidization processes that occurred in this Chloridoideae lineage during the last 10-25 MYs. The mechanisms underlying this chromosome number change suggest descending dysploidy ($n = 20$ to $n = 15$) through chromosomal repatterning contributing to cytological diploidization[45,46]. Descending dysploidy affecting polyploid genomes was reported as a more widespread mechanism than previously thought since the development of molecular cytogenetics, combined with comparative genomics and phylogenomic approaches[47,48]. Brassicaceae are particularly well-investigated with this regard, this family exhibiting multiple basic numbers resulting from independent cycles of polyploidization followed by genetic and genomic diploidization[49–51]. In grasses, descending dysploidy via nested chromosome fusions was found common in several subfamilies (e.g. Pooideae: *Brachypodium*[52], Panicoideae: *Saccharum*[53]). In the Chloridoideae subfamily, the ancestral grass genome underwent chromosome number reduction from $n = 12$ to $n = 10$[54] and more recent descending dysploidy events were identified in *Cynodon*[55] and *Eleusine*[56]. In *Sporobolus*, although the various basic chromosome numbers reported in the literature[13] suggest chromosomal restructuring events, to our knowledge descending dysploidy was not previously documented at the genomic scale in this genus containing worldwide invasive species and most particularly in section *Spartina* where it seems to have occurred between WGD1 and WGD2, thus reshuffling the ancestral genome. No species from the *Spartina* clade are known with 2n = 30 chromosomes (that could have performed regular meiosis as diploid with 15 chromosome pairs), so we can speculate that WGD2 occurred rapidly following this reduction and/or that these cytotypes might have been eliminated in natural populations at the time of their formation. Autopolyploid or allopolyploid origin can be hardly distinguished in mesopolyploids where related diploids are not available, and when considering the various long-term evolutionary fates of the duplicated genomes. The absence of known 2n = 30 differentiated species that could have hybridized before WGD2, and the identical structure of the A1 and A2 or B1 and B2 subgenomes respectively would suggest possible autopolyploidy. The estimated divergence between these recently duplicated subgenomes (WGD2: 2.1–6.2 MYA) might then represent the time elapsed since cytological diploidization. However, allopolyploidy could not be totally ruled out considering the possibility that differentiated 2n = 30 populations might have formed in the past and gone extinct. The structural similarity between the subgenomes could then be viewed as a result of preferential pairing and disomic inheritance (cytological diploidization) associated with the sequence divergence between parental subgenomes.

When considering molecular dating, the range of estimated divergence time between these species (2.6–6.8 MYA, this study, 2-4 MYA from cpDNA[39]) and that of WGD2 appear overlapping, which suggests that WGD2 and speciation might have occurred successively in a relatively narrow window of evolutionary time.

The speciation event leading to the modern *S. maritimus* and *S. alterniflorus* species was accompanied by chromosome number difference 2n = 60 and 62, respectively. Here, we elucidated the nature of the polysomy (2n = 60 + 2) in *S. alterniflorus* which was early reported in native populations from Canada, USA (Massachusetts) and introduced populations in England[36]. We showed that this difference did not result from nondisjunction of homologous chromosomes at meiosis that would have duplicated one chromosome pair, but rather, results from chromosomal repatterning.

From the phylogenetic perspective, the ancestral chromosome number state (i.e. 30 or 31) in the *S. maritimus* - *S. alterniflorus* clade (*Sporobolus* sect. *Spartina* subsect. Alterniflori) cannot be ascertained, as the sister *Sporobolus* lineages have 2n = 40 (n = 20) chromosomes[13,37] and there is no known sister lineage with 2n = 60 or 2n = 62 species. The chromosomal repatterning between the two genomes found here can be readily explained by a non-reciprocal translocation in the 2n = 60 chromosome that led to an additional chromosome pair (chromosome 31) as displayed in Fig. 3. In this proposed scenario, $n = 30$ would represent the ancestral state that evolved to $n = 31$ (derived state), through ascending dysploidy ("$n + 1$" hypothesis). In this scenario, WGD1 (that led to the evolution of $n = 10$ to $n = 20$), was followed by a base chromosome number reduction to 15 which could have resulted from five chromosome fusion events, and was subsequently duplicated by WGD2, as observed in the modern *S. maritimus* genome. A non-reciprocal translocation led to the additional chromosome 31 and to the observed chromosomal restructuration in *S. alterniflorus* (Fig. 3B, Supplementary Fig. 10). This latter chromosome presents a unique combination of HORs compared to other *S. alterniflorus* chromosomes, with the loss of the widely dispersed putatively centromeric 147-bp repeat (on most chromosomes of both species) and the spread of the 370-bp satellite (invading the *S. alterniflorus* genome). This 370-bp repeat was particularly abundant in

Table 1 | Functional divergence in restructured homologous chromosomal regions between *S. maritimus* and *S. alterniflorus*

GO term	*S. maritimus* (unshared on Scaf20-Scaf22)	Shared	*S. alterniflorus* (unshared on Chr31)
Biological process	Arabinan catabolic process*	Cell population proliferation	Cellular biosynthetic process
	Chalcone biosynthetic process*	Defense response to insect	Defense response to fungus
	Lipid biosynthetic process*	Pollen tube growth	Leaf senescence
	Pattern recognition receptor signaling pathway*	Regulation of anthocyanin biosynthetic process	Polysaccharide biosynthetic process
	Pollen tube development*	Response to light intensity	Regulation of biological process
	Reproduction*	Xylan catabolic process	Signal transduction
Cellular component	Chromosome	Apical plasma membrane	Cytosolic ribosome
	Extracellular exosome	Cell plate	DNA polymerase III complex
	Extrinsic component of plasma membrane	DNA replication factor C complex	Eukaryotic translation initiation factor 2B complex
	Nucleoplasm	Exocyst	Integral component of endoplasmic reticulum membrane
	Pollen tube tip	Plastoglobule	Intracellular anatomical structure
	Root hair tip	Spliceosomal complex	Ubiquitin ligase complex
Molecular function	α-L-arabinofuranosidase activity*	Acyltransferase activity	α-mannosidase activity
	β-glucosidase activity*	ADP binding	Amino acid binding
	Chitinase activity*	Carbon-nitrogen ligase activity	Carboxypeptidase activity
	Lysozyme activity*	Fatty acid elongase activity	Hydrolase activity. hydrolyzing *O*-glycosyl compounds
	Ribosomal large subunit binding*	Hydroquinone:oxygen oxidoreductase activity	*O*-methyltransferase activity
	Xylan 1,4-β-xylosidase activity*	Lipid binding	Ribonucleoside triphosphate phosphatase activity

Shared and species-specific GO terms identified in the corresponding restructured homologous chromosomal regions are shown. The GO terms that contain smaller (one-sided) *p*-value are shown, and asterisks * represent *p*-adjusted value < 0.05. The total GO terms are included in Supplementary Data 1.

S. alterniflorus subtelomeric chromosomal regions and it was found in both internal and distal regions of chromosome 31 (Supplementary Fig. 5), so we might speculate that such repeats could potentially be recruited as centromeric repeats in *S. alterniflorus* chromosome 31. Alternatively, descending dysploidy from $n = 31$ to $n = 30$ (scenario two, Supplementary Fig. 11) could have occurred, for instance if base chromosome number reduction between WGD1 and WGD2 evolved from $n = 20$ to $n = 16$ (e.g. through four chromosomal fusion events), leading to an ancestral genome of $n = 32$, which underwent descending dysploidy (from $n = 32$ to $n = 31$ involving one chromosomal fusion (Supplementary Fig. 11). However, in this case, two independent evolutionary events would be needed in the *S. alterniflorus* and *S. maritimus* lineages, respectively. According to our genomic comparisons and synteny analyses (Fig. 2), S. *maritimus* would have resulted from an additional fusion (resulting in $n = 30$), whereas *S. alterniflorus* would have undergone an additional non-reciprocal translocation (between *S. alterniflorus* chromosomes 15 and 4, Supplementary Fig. 11). This latter scenario, involving seven chromosomal restructuring events (including three post-WGD2), is less parsimonious than the previous one (which involved six evolutionary events, including only one restructuring event post-WGD2, Supplementary Fig. 10). This second ("*n*-1") scenario seems also unlikely as it would imply that the two distinct fusion events after WGD2 affected recurrently the same chromosome pairs (Supplementary Fig. 11). Additionally, this scenario would require the repatterning of HORs of the ancestral Chr31 translocated regions to *S. maritimus* homologous scaffolds with a reversion to 147-bp putative centromeric repeats. Also, no species from the *Spartina* clade have been reported with $2n = 32$ or $2n = 64$ ($x = 16$) chromosome number, and the presence of $2n = 60$ would rather suggest that WGD2 occurred after reduction to $n = 15$. Altogether, our results suggest that although the ancestral genome structure predating the divergence between *S. alterniflorus* and *S. maritimus* is not known, the 30 + 1 evolutionary scenario proposed here would represent a reasonable hypothesis.

The 30 to 31 chromosome number change that can be readily explained by one non-reciprocal translocation (instead of successive additional events over time) explains the biological isolation between the two species, which is also supported by the similar time range estimated between WGD2 and the *S. maritimus* - *S. alterniflorus* divergence. The WGD2 event occurring before the non-reciprocal translocation is consistent with the complete 31 bivalent chromosome pairing at meiosis in *S. alterniflorus*[35]. In North-America, two species share the $2n = 62$ chromosome number: *S. alterniflorus* (native to the North Atlantic American coast[26]) and its sister species *S. foliosus* endemic to the Pacific coast of California and Mexico[57]. These two species are actually weakly divergent genetically[37,38], and hybridized recurrently in California where *S. alterniflorus* was introduced, forming fertile and introgressant hybrids[15]. This makes questionable the biological species status of *S. foliosus* which most likely derived from an introduced ancestral lineage of *S. alterniflorus* (carrying the 60 + 2 chromosomal structure) on the Pacific coast that formed what are now considered as "native" populations of *S. foliosus*. *S. maritimus* which kept the $2n = 60$ genomic structure, is native to the European and African Atlantic coasts, and diverged 2.6–6.8 MYA from the ancestral North American Atlantic *S. alterniflorus* lineage following westward long-distance dispersal before the occurrence of the translocations that provided the additional chromosome pair in the native American *S. alterniflorus* and *S. foliosus*. This scenario is supported by the absence of reported cytotypes of $2n = 60$ for *S. alterniflorus* populations in their native and introduced ranges.

As a result of chromosomal restructuring, biological, then geographical isolation of *S. alterniflorus* and *S. maritimus* had consistent phenotypic and genetic differentiation with important ecological consequences. These species exhibit marked different morphologies[43],

mating systems and population biology: *S. alterniflorus* is a predominantly wind-pollinated outcrossing species with high seed set and variable levels of selfing in native and introduced populations, which has contributed to the spread *S. alterniflorus* populations[58,59]. High genetic diversity has been reported within and among *S. alterniflorus* populations[60–63]. Genetic mixture among source populations exposed to differential selective pressures allowed the spectacular expansion across a large latitudinal gradient of the populations introduced to China that evolved competitive traits, such as early flowering time, great competitive ability and greater plant biomass[42]. *S. maritimus* is believed to have evolved self-sterility[35], it produces viable pollen but very low seed set[64] and propagates mainly by vegetative means, which results in genetically depauperate populations[65]. Interestingly, we found that the restructured chromosomal regions between *S. maritimus* and *S. alterniflorus* were enriched in genes involved in pollen tube development, which could be related to the differential evolution of reproductive traits in these species. *S. alterniflorus* is considered as an invasive species in several continents[66] whereas *S. maritimus* is restricted to its native area along European and African coasts where it seems to be declining in its northern range limit. Both species colonize low saltmarsh habitats and mudflats, but *S. alterniflorus* grows on a larger range of environmental conditions, from brackish waters in estuaries to more frequently flooded or high tidal zones where it may be exposed to greater salt and drought stresses. These differential ecological and physiological traits are in direct line with differential regulatory (e.g. DNA methylation[18], small RNAs[22]) and gene expression pattern evolution[24] that result in higher salt and xenobiotic tolerance in *S. alterniflorus*[9,24,25]. Whether genes involved in defense response to herbivores and to flooding that appear enriched in the restructured chromosomal regions are involved in such physiological and ecological divergence is interesting to be further investigated.

Genetic isolation between *S. alterniflorus* and *S. maritimus* resulted in 1.30–3.4% nucleotide divergence as estimated from our analyses (Supplementary Fig. 8), and notably in differential repetitive sequence evolution. The analysis of LTR elements insertion time revealed an overall shared dynamic, but with a differential retention and expansion of repeats (e.g. *Gypsy* elements) between species. Our findings are consistent with previous analyses on repeated sequences in *Spartina* genomes[23] which found a shared transposition burst between these two species. Additionally, these authors identified a 370 bp-long satellite repeat mostly found in subtelomeric regions on one chromosome arms in 40 chromosomes of *S. alterniflorus* and only in 4 chromosomes of *S. maritimus*[23]. Two chromosomes of *S. alterniflorus* displayed this repeat in both arms of the chromosomes and were hypothesized to represent the extra-chromosome pair of *S. alterniflorus*. The annotation of this repeat on the assembled *S. alterniflorus* genome (Supplementary Fig. 5) agrees with the physical distribution of the repeats previously detected by FISH analysis[23], and indicates that chromosome 24 exhibits this sequence in both arms. However, chromosome 24 is not the extra-chromosome of *S. alterniflorus* which is actually chromosome 31.

The chromosome restructuring which accompanied divergence between the *S. alterniflorus* and *S. maritimus* lineages might have resulted in the biological isolation of these two species, as well-illustrated in the two independently formed hybrids (*S. x townsendii* and *S. x neyrautii*) which are both sterile[14]. Interestingly these two hybrids exhibited 2n = 62 chromosomes, suggesting that the chromosome pair 31 was transmitted "*en bloc*" in both events. Our investigations of the sequence composition of chromosome 31 indicate no particular transposable element dynamics compared to the other chromosomes, but the detected enrichment of genes involved in meiotic recombination (Supplementary Data 1) could help further exploration and understanding of why a chromosome pair did not segregate at meiosis. This chromosome pair, which resulted from ancestral chromosome restructuring, exhibits low amounts of putative centromeric repeats as discussed above, which could also contribute to chromosomal missegregation in *S. alterniflorus* meiosis (Supplementary Fig. 4A).

In summary, the availability and comparative analyses of the *S. alterniflorus* and *S. maritimus* genomes not only revise the evolutionary history of these two foundation species but also underscore the significance of understanding the evolutionary dynamics of hybrids for effective environmental management and legislation[67]. This study reveals the particular genome dynamics where an ancestral duplicated genome ($n = 2x = 20$) got diploidized resulting in a genome with an unexpected base chromosome number ($n = 15$) that duplicated again 2.1–6.2 MYA to form a tetraploid lineage ($2n = 4x = 60$). This appears to have been rapidly followed by chromosome restructuring that resulted in the divergence between the modern *S. maritimus* (2n = 60) and *S. alterniflorus* (2n = 62) genomes. Our findings reveal consequences of their recent hybridization and their successful derived neopolyploid *S. anglicus*, which appears then to be a modern octoploid ($2n = 8x = 124$) and not dodecaploid as previously thought[17]. This provides invaluable understanding of the genome composition in this system, and enables to explore more accurately important processes such as subgenome dominance, genome fractionation following superimposed paleo-, meso-, and neo-polyploidization events and their functional and ecological impacts in modern species. The assembled reference genomes of the *Spartina* clade presented here, provide genome composition and annotation, and contribute to effective strategies for saltmarsh restoration in native habitats and for managing invasive populations. Our grasp of the genetic and evolutionary background of hybrids and derived allopolyploid can profoundly influence environmental management decision-making and legislative frameworks when hybrids are involved, ensuring that conservation efforts are both scientifically informed and forward-looking[67].

Methods

Plant materials

S. maritimus was sampled at the Presqu'île du Verdon (Morbihan, France 47°43'11.0"N 3°09'19.3"W). Plants were subsequently transplanted in the greenhouse at the University of Rennes (France) and maintained until analyzed. *S. maritimus* voucher is deposited in the REN Herbarium at University of Rennes under (ID *REN015692)*. The plant ploidy level and genome size were assessed by flow cytometry[23].

S. alterniflorus was sampled in Sapelo Island (Georgia, USA), a source location from which plants were introduced to China[42]. The collected sample was subsequently grown in the greenhouse at Fudan University (Shanghai, China, 31°3'68.9"N 121°50'93.7"E). *S. alterniflorus* voucher ID is *USSA13*. Chromosome number was checked and genome size of *S. alterniflorus* was estimated using flow cytometry. Methods regarding DNA extraction, sequencing, genome assembly and annotation for *S. alterniflorus* were presented in Hao et al. [42]. The methodology for *S. maritimus* is detailed below.

S. maritimus DNA extraction, genome sequencing and optical mapping

High molecular weight DNA extraction from young fresh leaves of *S. maritimus* was performed using the Macherey Nagel Plant Nucleospin kit following instructions from the manufacturer. Estimation of DNA fragment sizes was performed using the Biorad CHEF-DR® II Pulsed Field Electrophoresis System. DNA extraction for Optical Mapping (BionanoSaphir) was performed after cell & subcellular fractionation with Percoll® (Sigma-Aldrich) (i) at the ECOBIO lab using the protocol developed by Zhang et al.[68] and (ii) at the Genoscope, using the Kit Bionano Prep High Polyphenols Plant Tissue DNA Isolation Protocol. Whole genome sequencing was achieved by combining paired-end Illumina® sequencing (PE250 bp) on a NovaSeq 6000 and the Oxford Nanopore technology (5 MinION and 3 PromethION flow cells) cumulating 370 Gb of short reads (200x coverage considering a 1.795

Gb-large genome) and 148 Gb of long reads (82x coverage). Optical map was obtained using the Bionano Saphyr instrument. The labeling protocol was performed following instructions from the manufacturer and the preparation was loaded on a chip as recommended by Bionano Genomics.

S. maritimus Genome assembly

Genome size and heterozygosity rate were estimated using Genomescope2[69]. Different k-mer values were tested to reach a genome size fitting with flow cytometry estimations. With a k-mer size of 31 bp, Genomescope2 estimated the genome size at 1473 Mb and the heterozygosity rate at 0.05%, while using a smaller k-mer size of 21-bp, resulted in the detection of two sets of sequences diverging by ~6% (and a genome size of 691 Mb). Nanopore reads were assembled using three different assemblers: SMARTdenovo[70], Redbean[71], Flye[72]. Smartdenovo was launched with -k 17 and -c 1 to generate a consensus sequence. Redbean was launched with '-xont -X5000 -g1500m' and Flye with '-g 1500m'. Based on the contiguity and the fact that we also have an optical map to organize and validate output contigs, we selected the Flye assembly which has a cumulative size of 2400 Mb with 17,791 contigs and a N50 of 483 Kb. This assembly was polished three times using Racon[73] and three times using Pilon[74] and Illumina short-reads. The BspQI optical map was generated using the produced molecules and software provided by Bionano Genomics (BNG). The assembly pipeline developed by BNG with the following two options: "add pre-assembly" and "non haplotype without extend and split". Bionano solve and tools (v1.3) was used to generate the hybrid scaffolds. Finally, artifactual duplications (negative gaps) were removed using BisCoT[75], followed by a polishing step with short reads using Hapo-G[76]. The final assembly consisted of 69 scaffolds with a cumulative size of 1.6 Gb. The completeness of genome assembly was assessed with BUSCO 5.2.2[77], on both eukaryote and angiosperm datasets. Homologous regions of *S. maritimus* and *S. alterniflorus* genomes were represented with Circos[78], including conserved syntenic blocks, and the distribution of annotated genes and repeats of the *S. maritimus* genome calculated by 100kb-windows.

Annotations

For *S. maritimus*, the annotation of protein-coding genes was performed by gene model predictions GeneMarkE-S[79], transcript-based predictions from RNA-seq data[24,25,40] with TransDecoder v2.0[80] and mapping using Stringtie v.1.3.3[81]. Spliced alignments for both predicted proteins and CDS were performed with exonerate[82] and all predictions being combined with EVM[83]. Homology searches were done by BLASTp[84] to a database of Poaceae and *Arabidopsis thaliana* proteins, and previously assembled reference transcriptomes in *Spartina*[24,25,40,41]. The repeat content was assessed using de novo predictions obtained with RepeatExplorer for five *Sporobolus* species[23] and a Poaceae-repeat database annotated with RepeatMasker v1.0.6[85]. Tandem Repeat Annotations were performed using TRASH to identify higher order repeats and putative centromere associated satellites[86]. We also investigated subgenome dosage in *S. maritimus* and *S. alterniflorus* by mapping short-reads back to the corresponding assembled genome with minimap2[87] (parameters: "-I 3 G --sam-hit-only -a -x sr") and calculating coverage using mosdepth[88] (parameters: 50Kb windows; "--by 50000 -n -i 2 -Q 10 -x").

Homology and synteny searches within and among genomes

To detect duplicated genomic regions in the *Sporobolus* genomes, we first performed comparative analyses at the genomic scale using a RBH (Reciprocal Blast Hit) procedure to keep all the reciprocal hits, considering the ploidy level of the concerned species. Self-BLASTn and interspecific BLASTn alignments (BLAST, v2.9.0[89]) were carried out using *S. maritimus*, *S. alterniflorus* and *Oryza sativa* v7.0[90] CDS predicted sequences. Significant hits were filtered out with an e-value < 1e-5, an identity ≥ 70%, an alignment length ≥ 60 nucleotides, and removal of repeated sequences. An intragenomic analysis in *O. sativa* was carried out to set parameters improving the detection of both ancient duplications (deriving from the *rho* event shared by Poaceae) and recent WGD events within *Sporobolus* genomes. A second complementary approach was used to search for homologous sequences (1) within *S. maritimus* (2) within *O. sativa* and (3) between *S. maritimus* and *O. sativa*, with the OrthoFinder2 program[91] using default settings (diamond, dendroblast and fastme). Five other genomes were added to this analysis (*Brachypodium distachyon*, *Setaria italica*, *Sorghum bicolor*, *Eragrostis tef* and *Oropetium thomaeum*) in order to obtain more reliable groups of orthologs.

The MCScanX tool[92] was used to search for synteny within RBH datasets for intragenomic analyses of *S. maritimus*. Default parameters were used (e-value < 1e-05, match score ≥ 50, match size ≥ 5, overlap window = 5, gap penalty = -1 and max gaps = 25). MCScan (Python version) was also used to infer the pairwise synteny regions for *S. alterniflorus*. Briefly, syntenic regions were identified using 'jcvi.compara.catalog' module with '--no_strip_names' and 'jcvi.compara.synteny' module with '--minspan = 30'[93]. A search for conserved syntenic blocks using home-made python scripts was carried out from RBH and Ks data (see below) within *S. maritimus* and *S. alterniflorus* genomes. Gene pairs with Ks values below 0.01 and ≥ 0.13 were excluded to focus specifically on syntenic blocks resulting from the most recent WGD event. Orthologous syntenic blocks were then retrieved between the chromosomes of *S. alterniflorus* and the scaffolds of *S. maritimus* as following: syntenic blocks were only considered when containing at least five pairs of homologous genes without gaps exceeding 25 genes, and multiple copy genes were discarded. Karyotype visualization was performed using the python/turtle module where 64 *S. maritimus* scaffolds were employed to reconstruct the 30 *S. maritimus* "pseudo-chromosomes". The "WGD_Tracker" pipeline used for these analyses (RBBH search, Ks calculations, synteny search, dotplot and karyotype graphic representations) is available at https://github.com/MorganeMilin/WGD_Tracker[94]. It is important to note that since the *S. maritimus* pseudo-chromosomes were constructed based on the *S. alterniflorus* genome assemblies, we cannot exclude the possibility that recombination occurs at scaffold breaks, and subsequently need to be cautious when examining these regions. Syntenic relationships focusing on the restructured chromosomes between the two species were visualized using the 'jcvi.graphics.karyotype' module of the JCVI tool[95]. Functional annotation of protein-coding genes was performed for *S. alterniflorus* and *S. maritimus* using the databases TrEMBL[96], eggNOG[97] and InterPro[98]. GO enrichment analyses were performed for the two species at both the restructured region and whole genome level using the R package clusterProfiler v.4.6.0[99]. GO analysis was performed using the enricher function from the clusterProfiler package, employing a hypergeometric test (default one-sided) to assess enrichment of GO terms, with False Discovery Rate correction (Benjamini-Hochberg) for multiple comparisons. Exact *p*-values, *p*-adjusted values (with a cutoff of 0.05), and *q*-values for each term are available in the Supplementary Data 1. All codes used for GO enrichment analyses were submitted to GitHub (https://github.com/tytrhr/GO_enrichment.git).

Divergence between duplicated subgenomes

To estimate the divergence between homeologous subgenomes, synonymous substitutions rates (Ks) were calculated for each duplicated gene pair that were aligned using MACSE[100,101], with default parameters. Ks were estimated using the Nei and Gojobori model[102] with the codeml program included in the PAML package[103]. The expectation-maximization (EM) algorithm was applied to fit mixtures of normal distributions and to estimate standard deviation to Ks data using the normalmixEM function in the mixtools R package[104]. Divergence time (T in years) between duplicates resulting from WGD events

was calculated as

$$T = Ks/(2 \times (6.5 \times 10^{-9})) \quad (1)$$

where 6.5×10^{-9} substitutions per site per year is the commonly used reference of monocot substitution rate[105]. Each peak mode associated with standard deviation values enabled to estimate the range of each event.

The LTR_retriever tool was used for the accurate identification of LTR retrotransposons in *S. maritimus* and *S. alterniflorus*[106]. The insertion time of transposons was calculated as

$$T = (1 - \text{identity})/(2\text{xmu}) \quad (2)$$

where "identity" corresponds to the identity calculated by LTR_retriver for each element and "mu" corresponds to the mutation rate (1.3×10^{-8})[107].

Reporting summary

Further information on research design is available in the Nature Portfolio Reporting Summary linked to this article.

Data availability

The Illumina, Oxford Nanopore, and Bionano Genomics sequencing reads of *S. maritimus* are available in the European Nucleotide Archive database under accession PRJEB73506. Genome assembly and annotation of *S. maritimus* are available at Figshare [https://figshare.com/projects/Sporobolus_maritimus_genome_annotation/235733]. Previously reported *S. alterniflorus* data[42] are available in the National Genomics Data Center database under accession PRJCA016449. Source data are provided with this paper.

Code availability

Codes for data cleaning and analysis (WGD_Tracker pipeline mentioned in Methods section) are available at Github [https://github.com/MorganeMilin/WGD_Tracker]. Codes for the GO enrichment analyses are also available at GitHub [https://github.com/tytrhr/GO_enrichment.git].

References

1. Wendel, J. F. The wondrous cycles of polyploidy in plants. *Am. J. Bot.* **102**, 1753–1756 (2015).
2. Soltis, D. E. et al. The Early Stages of Polyploidy: Rapid and Repeated Evolution in *Tragopogon*. in *Polyploidy and Genome Evolution* (eds. Soltis, P. S. & Soltis, D. E.) 271–292 (Springer Berlin Heidelberg, Berlin, Heidelberg). https://doi.org/10.1007/978-3-642-31442-1_14 (2012).
3. Van De Peer, Y., Mizrachi, E. & Marchal, K. The evolutionary significance of polyploidy. *Nat. Rev. Genet.* **18**, 411–424 (2017).
4. Doyle, J. J. & Coate, J. E. Polyploidy, the Nucleotype, and Novelty: The Impact of Genome Doubling on the Biology of the Cell. *Int. J. Plant Sci.* **180**, 1–52 (2019).
5. Freeling, M. et al. Fractionation mutagenesis and similar consequences of mechanisms removing dispensable or less-expressed DNA in plants. *Curr. Opin. Plant Biol.* **15**, 131–139 (2012).
6. Wang, X., Morton, J. A., Pellicer, J., Leitch, I. J. & Leitch, A. R. Genome downsizing after polyploidy: mechanisms, rates and selection pressures. *Plant J* **107**, 1003–1015 (2021).
7. Van De Peer, Y., Ashman, T.-L., Soltis, P. S. & Soltis, D. E. Polyploidy: an evolutionary and ecological force in stressful times. *Plant Cell* **33**, 11–26 (2021).
8. Fox, D. T., Soltis, D. E., Soltis, P. S., Ashman, T.-L. & Van De Peer, Y. Polyploidy: A Biological Force From Cells to Ecosystems. *Trends Cell Biol* **30**, 688–694 (2020).
9. Cavé-Radet, A., Salmon, A., Lima, O., Ainouche, M. L. & El Amrani, A. Increased tolerance to organic xenobiotics following recent allopolyploidy in *Spartina* (Poaceae). *Plant Sci* **280**, 143–154 (2019).
10. Tossi, V. E. et al. Impact of polyploidy on plant tolerance to abiotic and biotic stresses. *Front. Plant Sci.* **13**, 869423 (2022).
11. Ainouche, M. L. et al. Hybridization, polyploidy and invasion: lessons from *Spartina* (Poaceae). *Biol. Invasions* **11**, 1159–1173 (2009).
12. Te Beest, M. et al. The more the better? The role of polyploidy in facilitating plant invasions. *Ann. Bot.* **109**, 19–45 (2012).
13. Peterson, P. M., Romaschenko, K., Arrieta, Y. H. & Saarela, J. M. A molecular phylogeny and new subgeneric classification of *Sporobolus* (Poaceae: Chloridoideae: Sporobolinae). *Taxon* **63**, 1212–1243 (2014).
14. Ainouche, M. L., Baumel, A. & Salmon, A. *Spartina anglica* C. E. Hubbard: a natural model system for analysing early evolutionary changes that affect allopolyploid genomes: Evolution of *Spartina anglica*. *Biol. J. Linn. Soc.* **82**, 475–484 (2004).
15. Strong, D. R. & Ayres, D. R. Ecological and Evolutionary Misadventures of *Spartina*. *Annu. Rev. Ecol. Evol. Syst.* **44**, 389–410 (2013).
16. Bortolus, A. et al. Supporting *Spartina*: as a distinct solid genus. *Ecology* **100**, e02863 (2019).
17. Ainouche, M. et al. Polyploid Evolution in Spartina: Dealing with Highly Redundant Hybrid Genomes. In *Polyploidy and Genome Evolution* (eds Soltis, P. & Soltis, D.) 225–243 (Springer, Berlin, Heidelberg, 2012).
18. Salmon, A., Ainouche, M. L. & Wendel, J. F. Genetic and epigenetic consequences of recent hybridization and polyploidy in *Spartina* (Poaceae). *Mol. Ecol.* **14**, 1163–1175 (2005).
19. Chelaifa, H., Monnier, A. & Ainouche, M. Transcriptomic changes following recent natural hybridization and allopolyploidy in the salt marsh species *Spartina* × *townsendii* and *Spartina anglica* (Poaceae). *New Phytol* **186**, 161–174 (2010).
20. Rousseau, H. et al. Evolution of DMSP (dimethylsulfoniopropionate) biosynthesis pathway: Origin and phylogenetic distribution in polyploid *Spartina* (Poaceae, Chloridoideae). *Mol. Phylogenet. Evol.* **114**, 401–414 (2017).
21. Ferreira De Carvalho, J. et al. Gene expression variation in natural populations of hexaploid and allododecaploid *Spartina* species (Poaceae). *Plant Syst. Evol.* **303**, 1061–1079 (2017).
22. Cavé-Radet, A. et al. Evolution of small RNA expression following hybridization and allopolyploidization: insights from *Spartina* species (Poaceae, Chloridoideae). *Plant Mol. Biol.* **102**, 55–72 (2020).
23. Giraud, D. et al. Evolutionary dynamics of transposable elements and satellite DNAs in polyploid *Spartina* species. *Plant Sci* **302**, 110671 (2021).
24. Giraud, D., Lima, O., Rousseau-Gueutin, M., Salmon, A. & Aïnouche, M. Gene and Transposable Element Expression Evolution Following Recent and Past Polyploidy Events in *Spartina* (Poaceae). *Front. Genet.* **12**, 589160 (2021).
25. Cavé-Radet, A. et al. Recent allopolyploidy alters *Spartina* microRNA expression in response to xenobiotic-induced stress. *Plant Mol. Biol.* **111**, 309–328 (2023).
26. Bortolus, A., Carlton, J. T. & Schwindt, E. Reimagining South American coasts: unveiling the hidden invasion history of an iconic ecological engineer. *Divers. Distrib.* **21**, 1267–1283 (2015).
27. Nie, M., Liu, W., Pennings, S. C. & Li, B. Lessons from the invasion of *Spartina alterniflora* in coastal China. *Ecology* **104**, e3874 (2023).
28. Maricle, B. R. & Lee, R. W. Aerenchyma development and oxygen transport in the estuarine cordgrasses *Spartina alterniflora* and *S. anglica*. *Aquat. Bot.* **74**, 109–120 (2002).

29. Redondo-Gómez, S. Bioaccumulation of heavy metals in. *Spartina*. *Funct. Plant Biol.* **40**, 913 (2013).
30. Ryan, A. B. et al. Identification and Genetic Characterization of Smooth Cordgrass for Coastal Wetland Restoration. *J. Aquat Plant Manage* **45**, 90–99 (2007).
31. Castillo, J. M. & Figueroa, E. Restoring Salt Marshes Using Small Cordgrass, *Spartina maritima*. *Restor. Ecol.* **17**, 324–326 (2009).
32. Baumel, A., Ainouche, M. L. & Levasseur, J. E. Molecular investigations in populations of *Spartina anglica* C.E. Hubbard (Poaceae) invading coastal Brittany (France). *Mol. Ecol.* **10**, 1689–1701 (2001).
33. Marchant, C. J. Corrected Chromosome Numbers for *Spartina x townsendii* and its Parent Species. *Nature* **199**, 929 (1963).
34. Roodt, R. & Spies, J. J. Chromosome studies in the grass subfamily Chloridoideae. I. Basic chromosome numbers. *Taxon* **52**, 557–583 (2003).
35. Marchant, C. J. Evolution in *Spartina* (Gramineae): II. Chromosomes, basic relationships and the problem of *S. x townsendii* agg. *J. Linn. Soc. Lond. Bot.* **60**, 381–409 (1968).
36. Marchant, C. J. Evolution in *Spartina* (Gramineae): III. Species chromosome numbers and their taxonomic significance. *J. Linn. Soc. Lond. Bot.* **60**, 411–417 (1968).
37. Baumel, A., Ainouche, M. L., Bayer, R. J., Ainouche, A. K. & Misset, M. T. Molecular Phylogeny of Hybridizing Species from the Genus *Spartina* Schreb. (Poaceae). *Mol. Phylogenet. Evol.* **22**, 303–314 (2002).
38. Fortune, P. M. et al. Evolutionary dynamics of *Waxy* and the origin of hexaploid *Spartina* species (Poaceae). *Mol. Phylogenet. Evol.* **43**, 1040–1055 (2007).
39. Rousseau-Gueutin, M. et al. The chloroplast genome of the hexaploid *Spartina maritima* (Poaceae, Chloridoideae): Comparative analyses and molecular dating. *Mol. Phylogenet. Evol.* **93**, 5–16 (2015).
40. Boutte, J. et al. Reference Transcriptomes and Detection of Duplicated Copies in Hexaploid and Allododecaploid *Spartina* Species (Poaceae). *Genome Biol. Evol.* **8**, 3030–3044 (2016).
41. Ferreira De Carvalho, J. et al. Transcriptome de novo assembly from next-generation sequencing and comparative analyses in the hexaploid salt marsh species *Spartina maritima* and *Spartina alterniflora* (Poaceae). *Heredity* **110**, 181–193 (2013).
42. Hao, Y. et al. Genomic and phenotypic signatures provide insights into the wide adaptation of a global plant invader. *Plant Commun.* 100820 https://doi.org/10.1016/j.xplc.2024.100820 (2024).
43. Mobberley, D. G. Taxonomy and distribution of the genus *Spartina*. 6866205 (Iowa State University, Digital Repository, Ames). https://doi.org/10.31274/rtd-180813-14058 (1956).
44. Doyle, J. J. & Egan, A. N. Dating the origins of polyploidy events. *New Phytol* **186**, 73–85 (2010).
45. Li, Z. et al. Patterns and Processes of Diploidization in Land Plants. *Annu. Rev. Plant Biol.* **72**, 387–410 (2021).
46. Lysák, M. A. & Schubert, I. Mechanisms of Chromosome Rearrangements. in *Plant Genome Diversity Volume 2: Physical Structure, Behaviour and Evolution of Plant Genomes* (eds. Greilhuber, J., Dolezel, J. & Wendel, J. F.) 137–147 (Springer Vienna, Vienna). https://doi.org/10.1007/978-3-7091-1160-4_9 (2013).
47. Mandáková, T. & Lysak, M. A. Post-polyploid diploidization and diversification through dysploid changes. *Curr. Opin. Plant. Biol.* **42**, 55–65 (2018).
48. Mayrose, I. & Lysák, M. A. The Evolution of Chromosome Numbers: Mechanistic Models and Experimental Approaches. *Genome Biol. Evol.* **13**, evaa220 (2021).
49. Lysák, M. A. et al. Mechanisms of chromosome number reduction in Arabidopsis thaliana and related Brassicaceae species. *Proc. Natl. Acad. Sci. USA* **103**, 5224–5229 (2006).
50. Lysák, M. A. & Koch, M. A. Phylogeny, Genome, and Karyotype Evolution of Crucifers (Brassicaceae) in: *Genetics and Genomics of the Brassicaceae. Plant Genetics and Genomics: Crops and Models* (eds. Schmidt, R., Bancroft, I.) 1–31 (Springer; New York, NY, USA). https://doi.org/10.1007/978-1-4419-7118-0_1 (2011).
51. Mandáková, T., Li, Z., Barker, M. S. & Lysák, M. A. Diverse genome organization following 13 independent mesopolyploid events in Brassicaceae contrasts with convergent patterns of gene retention. *Plant J* **91**, 3–21 (2017).
52. Lusinska, J. et al. Comparatively Barcoded Chromosomes of Brachypodium Perennials Tell the Story of Their Karyotype Structure and Evolution. *Int. J. Mol. Sci.* **20**, 5557 (2019).
53. Yu, F. et al. Chromosome-specific painting unveils chromosomal fusions and distinct allopolyploid species in the Saccharum complex. *New Phytol* **233**, 1953–1965 (2022).
54. Wang, F. et al. Sequence-tagged high-density genetic maps of Zoysia japonica provide insights into genome evolution in Chloridoideae. *Plant J.* **82**, 744–757 (2015).
55. Cui, F. et al. The genome of the warm-season turfgrass African bermudagrass (*Cynodon transvaalensis*). *Hortic Res* **8**, 93 (2021).
56. Devos, K. M. et al. Genome analyses reveal population structure and a purple stigma color gene candidate in finger millet. *Nat Commun* **14**, 3694 (2023).
57. Ayres, D. R. et al. Hybridization between invasive *Spartina densiflora* (Poaceae) and native *S. foliosa* in San Francisco Bay, California, USA. *Am. J. Bot.* **95**, 713–719 (2008).
58. Daehler, C. C. Variation in self-fertility and the reproductive advantage of self-fertility for an invading plant (*Spartina alterniflora*). *Evol. Ecol.* **12**, 553–568 (1998).
59. Davis, H. G., Taylor, C. M., Lambrinos, J. G. & Strong, D. R. Pollen limitation causes an Allee effect in a wind-pollinated invasive grass (*Spartina alterniflora*). *Proc. Natl. Acad. Sci.* **101**, 13804–13807 (2004).
60. Travis, S. E., Proffitt, C. E., Lowenfeld, R. C. & Mitchell, T. W. A Comparative Assessment of Genetic Diversity among Differently-Aged Populations of *Spartina alterniflora* on Restored Versus Natural Wetlands. *Restor. Ecol.* **10**, 37–42 (2002).
61. Bernik, B. M., Li, H. & Blum, M. J. Genetic variation of *Spartina alterniflora* intentionally introduced to China. *Biol. Invasions* **18**, 1485–1498 (2016).
62. Mounger, J. M. et al. Genetic and Epigenetic Differentiation Across Intertidal Gradients in the Foundation Plant *Spartina alterniflora*. *Front. Ecol. Evol.* **10**, 868826 (2022).
63. Shang, L. et al. High Genetic Diversity With Weak Phylogeographic Structure of the Invasive *Spartina alterniflora* (Poaceae) in China. *Front. Plant Sci.* **10**, 1467 (2019).
64. Infante-Izquierdo, M. D. et al. Fruit Set, Seed Viability and Germination of the European Native *Spartina maritima* in Southwest Iberian Peninsula. *Wetlands* **40**, 421–432 (2020).
65. Yannic, G., Baumel, A. & Ainouche, M. Uniformity of the nuclear and chloroplast genomes of *Spartina maritima* (Poaceae), a salt-marsh species in decline along the Western European Coast. *Heredity* **93**, 182–188 (2004).
66. Ainouche, M. & Gray, A. Invasive *Spartina*: lessons and challenges. *Biol. Invasions* **18**, 2119–2122 (2016).
67. Adam, P. The shock of the new? *Australasian Plant Conservation: journal Australian Network Plant Conservation* **24**, 19–21 (2015).
68. Zhang, M. et al. Preparation of megabase-sized DNA from a variety of organisms using the nuclei method for advanced genomics research. *Nat. Protoc.* **7**, 467–478 (2012).
69. Ranallo-Benavidez, T. R., Jaron, K. S. & Schatz, M. C. GenomeScope 2.0 and Smudgeplot for reference-free profiling of polyploid genomes. *Nat. Commun.* **11**, 1432 (2020).
70. Liu, H., Wu, S., Li, A. & Ruan, J. SMARTdenovo: a de novo assembler using long noisy reads. *Gigabyte* **2021**, 1–9 (2021).
71. Ruan, J. & Li, H. Fast and accurate long-read assembly with wtdbg2. *Nat. Methods* **17**, 155–158 (2020).

72. Kolmogorov, M., Yuan, J., Lin, Y. & Pevzner, P. A. Assembly of long, error-prone reads using repeat graphs. *Nat. Biotechnol.* **37**, 540–546 (2019).
73. Vaser, R., Sović, I., Nagarajan, N. & Šikić, M. Fast and accurate de novo genome assembly from long uncorrected reads. *Genome Res* **27**, 737–746 (2017).
74. Walker, B. J. et al. Pilon: An Integrated Tool for Comprehensive Microbial Variant Detection and Genome Assembly Improvement. *PLoS ONE* **9**, e112963 (2014).
75. Istace, B., Belser, C. & Aury, J.-M. BiSCoT: improving large eukaryotic genome assemblies with optical maps. *PeerJ* **8**, e10150 (2020).
76. Aury, J.-M. & Istace, B. Hapo-G, haplotype-aware polishing of genome assemblies with accurate reads. *NAR Genomics Bioinforma.* **3**, lqab034 (2021).
77. Manni, M., Berkeley, M. R., Seppey, M., Simão, F. A. & Zdobnov, E. M. BUSCO Update: Novel and Streamlined Workflows along with Broader and Deeper Phylogenetic Coverage for Scoring of Eukaryotic, Prokaryotic, and Viral Genomes. *Mol. Biol. Evol.* **38**, 4647–4654 (2021).
78. Krzywinski, M. et al. Circos: An information aesthetic for comparative genomics. *Genome Res* **19**, 1639–1645 (2009).
79. Lomsadze, A., Ter-Hovhannisyan, V., Chernoff, Y. O. & Borodovsky, M. Gene identification in novel eukaryotic genomes by self-training algorithm. *Nucleic Acids Res* **33**, 6494–6506 (2005).
80. Haas, B. J. & Papanicolaou, A. TransDecoder (Find Coding Regions Within Transcripts). https://github.com/TransDecoder/TransDecoder (2017).
81. Pertea, M. et al. StringTie enables improved reconstruction of a transcriptome from RNA-seq reads. *Nat. Biotechnol.* **33**, 290–295 (2015).
82. Slater, G. S. C. & Birney, E. Automated generation of heuristics for biological sequence comparison. *BMC Bioinformatics* **6**, 31 (2005).
83. Haas, B. J. et al. Automated eukaryotic gene structure annotation using EVidenceModeler and the Program to Assemble Spliced Alignments. *Genome Biol* **9**, R7 (2008).
84. Camacho, C. et al. BLAST + : architecture and applications. *BMC Bioinformatics* **10**, 421 (2009).
85. Chen, N. Using RepeatMasker to Identify Repetitive Elements in Genomic Sequences. *Curr. Protoc. Bioinforma.* **5**, 4.10.1–4.10.14 (2004).
86. Wlodzimierz, P., Hong, M. & Henderson, I. R. TRASH: Tandem Repeat Annotation and Structural Hierarchy. *Bioinformatics* **39**, btad308 (2023).
87. Li, H. Minimap2: pairwise alignment for nucleotide sequences. *Bioinformatics* **34**, 3094–3100 (2018).
88. Pedersen, B. S. & Quinlan, A. R. Mosdepth: quick coverage calculation for genomes and exomes. (2018).
89. Altschul, S. F. BLAST Algorithm. in *Encyclopedia of Life Sciences* (Wiley). https://doi.org/10.1002/9780470015902.a0005253.pub2 (2014).
90. Kawahara, Y. et al. Improvement of the *Oryza sativa* Nipponbare reference genome using next generation sequence and optical map data. *Rice* **6**, 4 (2013).
91. Emms, D. M. & Kelly, S. OrthoFinder: phylogenetic orthology inference for comparative genomics. *Genome Biol* **20**, 238 (2019).
92. Wang, Y. et al. MCScanX: a toolkit for detection and evolutionary analysis of gene synteny and collinearity. *Nucleic Acids Res* **40**, e49–e49 (2012).
93. Tang, H. et al. Synteny and Collinearity in Plant Genomes. *Science* **320**, 486–488 (2008).
94. Milin, M. WGD_Tracker (v1.0). *Zenodo* https://doi.org/10.5281/zenodo.14672010 (2025).
95. Tang, H., Krishnakumar, V. & Li, J. jcvi: JCVI utility libraries (v0.5.7). *Zenodo* https://doi.org/10.5281/zenodo.31631 (2015).
96. UniProt Consortium. "UniProt: a worldwide hub of protein knowledge.". *Nucleic Acids Res.* **47**, D506–D515 (2019).
97. Cantalapiedra, C. P. et al. eggNOG-mapper v2: functional annotation, orthology assignments, and domain prediction at the metagenomic scale. *Mol. Biol. Evol.* **38**, 5825–5829 (2021).
98. Blum, M. et al. The InterPro protein families and domains database: 20 years on. *Nucleic Acids Res.* **49**, D344–D354 (2021).
99. Wu, T. et al. clusterProfiler 4.0: A universal enrichment tool for interpreting omics data. *Innovation* **2**, 100141 (2021).
100. Ranwez, V., Harispe, S., Delsuc, F. & Douzery, E. J. P. MACSE: Multiple Alignment of Coding SEquences Accounting for Frameshifts and Stop Codons. *PLoS ONE* **6**, e22594 (2011).
101. Ranwez, V., Douzery, E. J. P., Cambon, C., Chantret, N. & Delsuc, F. MACSE v2: Toolkit for the Alignment of Coding Sequences Accounting for Frameshifts and Stop Codons. *Mol. Biol. Evol.* **35**, 2582–2584 (2018).
102. Nei, M. & Gojobori, T. Simple Methods for Estimating the Numbers of Synonymous and Nonsynonymous Nucleotide Substitutions. *Mol. Biol. Evol.* **3**, 418–426 (1986).
103. Yang, Z. PAML 4: Phylogenetic Analysis by Maximum Likelihood. *Mol. Biol. Evol.* **24**, 1586–1591 (2007).
104. Benaglia, T., Chauveau, D., Hunter, D. R. & Young, D. **mixtools**: Package for Analyzing Finite Mixture Models. *J. Stat. Softw.* **32**, (2009).
105. Gaut, B. S., Morton, B. R., McCaig, B. C. & Clegg, M. T. Substitution rate comparisons between grasses and palms: synonymous rate differences at the nuclear gene *Adh* parallel rate differences at the plastid gene *rbcL*. *Proc. Natl. Acad. Sci.* **93**, 10274–10279 (1996).
106. Ou, S. & Jiang, N. LTR_retriever: A Highly Accurate and Sensitive Program for Identification of Long Terminal Repeat Retrotransposons. *Plant Physiol.* **176**, 1410–1422 (2018).
107. Ma, J. & Bennetzen, J. L. Rapid recent growth and divergence of rice nuclear genomes. *Proc. Natl. Acad. Sci.* **101**, 12404–12410 (2004).

Acknowledgements

This work was conducted in the framework of a collaborative project (Interuniversity Convention) between the University of Rennes (France) and the Fudan University of Shanghai (China). The authors in China were financially supported by the National Key Research and Development Program of China (2022YFC2601100), the National Natural Science Foundation of China (31961133028), and the Department of Science and Technology of Yunnan Province (202405AS350011) to B.L. The authors in France acknowledge funding from UMR 6553 Ecology, Biodiversity and Evolution (Ecobio - Univ Rennes - CNRS to M.A., A.S., O.L.), support from University of Rennes (PhD grant to M. M.), support from Genoscope, CEA, France Génomique (ANR-10-INBS-09–08 to P.W), and from the CNRS - Rennes University funded International Research Network (IRN) Polyploidy and Biodiversity (POLYDIV) to M.A. C. Parisod and M. Beringer (U. Fribourg, CH) are thanked for helpful discussions on Ks analyses in polyploids. A. Leitch (QMU, London) and I. Leitch (RBG, Kew) are thanked for stimulating discussions on dysploidy and repetitive sequences. T. Fontaine and R. Bodiguel (UMR Ecobio, France) are thanked for help in maintaining the analyzed *S. maritimus* plants in the greenhouse.

Author contributions

A.S., Y.H., M.M., L.L., B.L., M.A. conceived & designed experiments. A.S., Y.H., M.M., L.L., B.L., M.A. performed experiments. A.S., Y.H., M.M., A.C.-R., D.G., B.I., C.B., J-.M.A., P.W., L.L., M.A. analyzed the data. O.L., C.C., K.L., P.W. contributed materials/analysis tools. M.A., A.S., Y.H., M.M., B.L., L.L. wrote the paper.

Competing interests

The authors declare no competing interests.

Additional information

Supplementary information The online version contains supplementary material available at https://doi.org/10.1038/s41467-025-56983-8.

Correspondence and requests for materials should be addressed to Bo Li, Lin-Feng Li or Malika Ainouche.

Peer review information *Nature Communications* thanks Alejandro Bortolus and the other, anonymous, reviewers for their contribution to the peer review of this work. A peer review file is available.